SPE Paper Number 93879

Monitoring Waterflood Operations: Hall's Method Revisited

D. B. Silin, SPE, Lawrence Berkeley National Laboratory and University of California, Berkeley; R. Holtzman, University of California, Berkeley; T. W. Patzek, SPE, University of California, Berkeley; J. L. Brink, SPE, ChevronTexaco Production Company

This paper was prepared for presentation at the 2005 SPE Western Regional Meeting held in Irvine, CA, U.S.A., 30 March – 1 April 2005.

Abstract

Hall's method is a simple tool used to evaluate performance of water injection wells. It is based on the assumption of steady-state radial flow. Besides historical injection pressures and rates, Hall's method requires information about the mean ambient reservoir pressure, p_e. In addition, it is assumed that the equivalent radius, r_e, of the reservoir domain influenced by the well is constant during the observation period. Neither p_e nor r_e are available from direct measurement.

Here we modify and extend Hall's plot analysis, calling it *slope analysis*. Our modification relies on the analysis of the variations of slope of the cumulative injection pressure versus cumulative injection volume. In particular, our slope analysis produces an estimate of the mean ambient reservoir pressure, and requires only the injection pressures and rates. Such data are routinely collected in the course of a waterflood. Note that the slope analysis method requires no interruptions of regular field operations.

The proposed slope analysis method has been verified with the numerically generated pressure and rate data, and tested in the field. In both cases it proved to be accurate, efficient, and simple. The obtained ambient reservoir pressure estimate can be used to correct the Hall plot analysis or to map the average reservoir pressure over several patterns or an entire waterflood project. Such maps can then be used to develop an efficient waterflood policy, which will help to arrest subsidence and improve oil recovery.

Introduction

Monitoring and control of performance of each individual well is an important component of successful oil recovery operations. The dramatic progress in information technology over the past decade has made it possible to collect and store huge volumes of high-quality production and injection data. These data, if appropriately interpreted, provide new insights into reservoir dynamics across multiple temporal and spatial scales. Therefore, efficient processing and interpretation of the high-frequency field measurements is a task of crucial importance to modern management of oil&gas recovery projects.

This paper deals with problems related to monitoring and control of waterflood operations. The necessity of collecting and processing numerous measurements was understood decades ago[1]. Recently, ChevronTexaco with participation of the Lawrence Berkeley National Laboratory and the University of California, Berkeley, developed a concept of field-wide surveillance and control of waterflood. This concept is being implemented in the Lost Hills oil field[2]. The work reported here is a part of this effort.

Waterflood performance in an entire oilfield results from the quality of each individual well. The global project objectives are derived from a field-scale analysis, such as inspection of satellite images for surface subsidence and uplift, and calculation of the fluid injection-withdrawal balance.[3] But the subsurface reservoir can only be accessed and controlled through wells. Therefore, it is critically important to have efficient methods for adequate assessment and monitoring of well performance, and for regular evaluation of reservoir conditions near the wellbore.

Traditional transient well tests have been used to evaluate the average near-wellbore formation transmissivity[4]. Such tests interrupt regular field operations. Their interpretation is based on analysis of transient effects taking place at time scales which are short relative to those of fluid injection and production. On one hand, unless there is a pipe-like circulation of injected fluid between an injector and the surrounding producers, the injection results in ever-changing reservoir conditions. On the other hand, these changes may be almost imperceptible over a typical observation time interval. Therefore, normal reservoir processes can be called quasi steady-state. In real life operations, short-time fluctuations of the injection pressures and rates at the well are inevitable. Separation of these short-time transient effects and long-time quasi steady-state processes is one of the most important tasks of well performance monitoring and diagnostics,[5-7] crucial to the information-driven oilfields of the future (the IFields).

Hall's method[8], see also[4], is an alternative to transient well test approach. Technically, it is very simple: just plot the time integral of injection pressure versus cumulative injection. The

integration automatically filters out short-time fluctuations. The slope of Hall's plot is interpreted as an indicator of the average well injectivity. As inputs, Hall's method only requires regular collection of injection rates and injection pressures, that are a part of routine waterflood operations. At normal conditions, the plot is a straight line and kinks on the plot should indicate changes of injection conditions. This method has been used extensively to assess success of a well treatment by comparing the slopes before and after the treatment[9, 10].

However, the simplicity of Hall's method can be deceiving. Rigorously speaking, a correct Hall plot interpretation requires information about the reservoir pressure at the distance equal to the mean influence radius of the well. If Hall's method is applied without *a priori* knowledge of the effective ambient reservoir pressure, then the conclusion that a kink in the plot is an indication of changes in the well injectivity can be wrong. Estimation of the reservoir transmissivity from the Hall plot is impossible, unless the influence radius is known and does not change during observations. Neither the reservoir pressure at the boundary of the influence domain nor the influence domain size is available from measurements. There is no evidence that the influence radius does not change after a well treatment or with changing injection rate. On the contrary, it is fair to assume that the variable well-operation conditions affect that radius.

Therefore, this paper revisits the Hall plot method and inspects its theoretical background. Application of Hall's analysis naturally extends to non-radial flow mode, but the quasi-steady-state flow assumption cannot be relaxed. In reality, the steady-state flow is inevitably disturbed by short-time (high-frequency) fluctuations of pressures and rates. It turns out that analysis of the Hall plot slope fluctuations, which we call *slope analysis*, reveals very important information about the effective reservoir pressure near the wellbore and the injectivity of the well. Like Hall's method, the slope analysis is very simple. As inputs, it only requires injection rate – injection pressure data. Information about the reservoir pressure is not required, but is derived instead as a part of the analysis. The dense well spacing in the Lost Hills oil field makes it possible to create maps of this effective reservoir pressure on different time intervals and to monitor the reservoir dynamics at the field scale. Comparison of these maps with satellite subsidence images provides valuable clues as how to make waterflood more efficient and to avoid unnecessary well failures. Jim, please look if you can elaborate here and here

The paper is organized as follows. First, we review the theoretical background of the Hall plot method. This part is included to make the presentation self-contained. Second, we demonstrate that Hall's method can lead to wrong conclusions if the reservoir pressure and the ratio between the influence radius and the effective wellbore radius are unknown. We do so by analyzing simulated data produced by a forward model of water injection. We use the methods[11,12] developed for well-test analysis, while accounting for regular field operations. Third, we propose a new well diagnostics method, called *slope analysis*. We illustrate this method using simulated data. In the concluding part, we verify our analysis against real injection data from the Lost Hills oil field.

Hall Plot: Theoretical Background

Hall plot is a tool to analyze steady-state flow at an injection well. Originally, it was based on the radial flow model [13]. According to this model,

$$p_w = p_e + \frac{\mu}{2\pi kH}\ln\frac{r_e}{r_w}Q \quad \text{.....(1)}$$

where p_w and p_e are the downhole wellbore pressure and reservoir pressure at r_e respectively, Q is the flow rate, μ is the injected fluid viscosity, k is formation permeability and H is the reservoir thickness. We neglect the compressibility of the reservoir fluid, so that the formation factor is equal to one. If necessary, it can be easily incorporated in Eq. (1) as an additional factor in front of Q. Also, we adopt the convention that injection flow rate is positive. To account for formation damage in close vicinity of the wellbore, or the skin effect, we assume some effective wellbore radius r_w[14]. The well influence zone is the zone near the wellbore where the fluid pressure changes appreciably due to the injection. In the radial flow model this influence zone is circular. The ratio r_e/r_w is between the wellbore radius and the radius of influence, *i.e.* the distance from the well to the part of the reservoir where the pressure can be considered undisturbed by the injection or held constant by other factors. In fact, equation (1) also holds true if the flow is not purely radial, in such a case the pressures have to be averaged [13].

Equation (1) is based on several assumptions. The fluid is homogeneous and incompressible. The reservoir is vertically confined and uniform, both with respect to the permeability and the thickness. The reservoir is horizontal and gravity does not affect the flow. Consequently, the flow is radial. During the entire time of observations, the pressure at the distance equal to r_e is constant, and this distance itself is constant as well. In practice, not all, if any, of these assumptions are strictly satisfied. The injection interval usually covers multiple zones of different permeability. The geometric structure of the flow can be distorted by formation heterogeneity, interference between wells, fractures, *etc.* Nevertheless, Eq. (1) is of great practical importance, and in many cases it adequately describes fluid injection assuming some effective mean formation parameters. The coefficient

$$b = \frac{\mu}{2\pi kH}\ln\frac{r_e}{r_w}, \quad \text{.....(2)}$$

or its inverse, is often used to characterize well performance. If the rates and pressures are almost constant over the observation time period, then

$$b = \frac{Q}{p_w - p_e} \quad \text{.....(3)}$$

that is b is the reciprocal of specific well injectivity[14]. Application of the last equation can be limited by the inevitable fluctuations of the pressure and rate, and the lack of information about the mean ambient pressure p_e.

Equation (1) can be integrated in time:

$$\int_{t_0}^{t}\left(p_w - p_e\right)d\tau = \int_{t_0}^{t}\left(\frac{\mu}{2\pi kH}\ln\frac{r_e}{r_w}Q\right)d\tau \quad \text{.....(4)}$$

Note that the upper limit of integration is variable. As t grows, the integration filters out short-time fluctuations providing a more robust procedure for evaluating the well performance parameter b.

Denote

$$\Pi(t) = \int_{t_0}^{t} p_w(\tau)\,d\tau \quad \text{and} \quad V(t) = \int_{t_0}^{t} Q(\tau)\,d\tau \quad \text{...(5)}$$

The Hall plot analysis is just plotting of the left-hand side of Eq. (4) versus the right-hand side, i.e., plotting $\Pi(t) - p_e t$ versus the cumulative injection volume $V(t)$. Clearly, at a constant ambient reservoir pressure p_e, and constant coefficient b, the plot is a straight line whose slope is equal to b. If the purpose of analysis is to compare formation transmissivity before and after well treatment, then the change of the slope, or the coefficient b, should be evaluated.

However, application of Eq. (4) still requires knowledge of p_e and an evidence of constancy of b during the time of observation. The following example illustrates the importance of this information. Imagine a well at quasi-static injection over a period of 6 days. Let both the reservoir pressure and parameter b be constant over this period of time. Assume that water is injected at a rate of 150 bbl/day and the wellbore injection pressure is 1500 psi during the first 4 days. The last two days, the rate is increased to 300 bbl/day by increasing injection pressure to 1700 psi. If the reservoir pressure is constant and equal p_e=1400 psi, we immediately obtain that the Hall plot is a straight line and b=0.5 psi-day/bbl. However, if we plot $\Pi(t) - p_e t$ versus cumulative injection volume $V(t)$ with an incorrect reservoir pressure estimate, then the plot has a break in the slope, Fig. 1. Thus, the only case when the Hall plot is a straight line with a variable injection rate is when the reservoir pressure p_e is known and its exact value is used in Eq. (4). If pressure p_e is unknown, even constant injection conditions may result in a Hall plot with a break in the slope. The magnitude of the slope change is a function of the discrepancy between the exact reservoir pressure and the pressure used in Eq. (4).

The original paper by Hall[8] provides an example of analysis of well data before and after a treatment assuming three different values of p_e. The same data yield three different slope changes after well treatment. The injection rate after the treatment has changed. Thus, to what degree the slope change is due to changes of the formation properties after the treatment and to what degree it is due to the lack of information about the reservoir pressure, cannot be ascertained from analyzing the plot alone.

The plot in Fig. 1 suggests that if the formation properties do not change and the reservoir pressure also remains the same, then the plot of Π(t)-p versus $V(t)$ is a straight line only if p=p_e. Thus, the formation pressure p_e can be estimated by selecting the value of p, such that the slope of the plot is constant. Below, a more elegant and robust reservoir pressure estimation procedure is discussed.

Some authors propose a simplified procedure, where the difference p_w-p_e is replaced with the wellhead pressure. The example above demonstrates that the uncertainty of such analysis is not negligible.

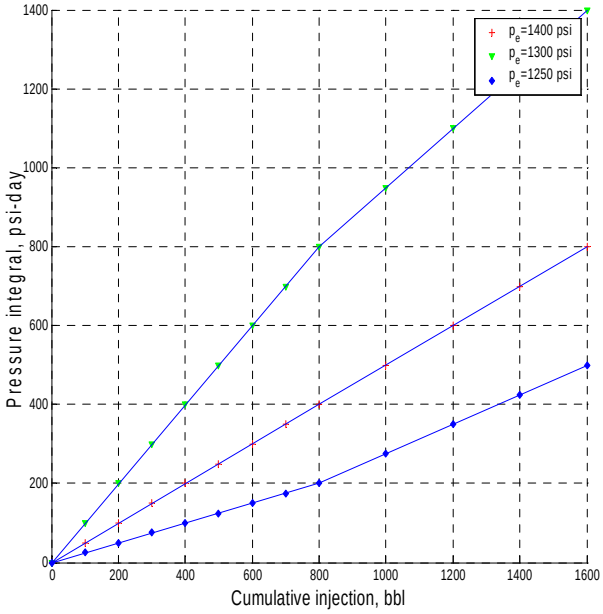

Fig. 1. Hall plot at constant formation properties, but with different reservoir pressures. The only straight line with the slope b=0.5 psi-day/bbl on this plot corresponds to the correct reservoir pressure 1400 psi.

Hall Plot: The Key Parameters

To investigate the impact of the ambient reservoir pressure and the radius of influence on Hall plot analysis, synthetic "reservoir data" were generated. The forward simulations were performed with a model used in well test analysis[11,12]. This model was built upon the classical Theis pressure diffusion equation to account for the impact of the steady-state component of flow driven by the near-wellbore reservoir pressure distribution. This model was selected as the tool for forward simulations because it uses assumptions, which are compatible with regular injection operations, where transient fluctuations are superimposed upon long-time steady-state flow. In this model, the reservoir parameters are represented as average effective quantities, exactly as in the Hall method. The model has been extensively verified against real field data. Well test analysis produces a good-quality injection pressure curve fit, which is stable with respect to the selection of the time interval. Analysis of regular operations data also produces consistent stable estimates[15].

Thus, the following procedure is used in this section. First, the various operation scenarios, *e.g.*, a step injection rate change, are simulated using the model[11,12]. Second, the result is plotted using the Hall plot method, and the signatures of the influence of different parameters are obtained. It turns out that analysis of the field data presented in the last section strongly confirms the simulation results.

The main equation used in model [11,12] is

$$p_w(t) = p_{0w} + A\int_{t_0}^{t} \frac{\exp\left(-\frac{B}{t-\tau}\right)}{t-\tau} Q(\tau)\, d\tau$$

$$+ AQ_{-1}\,\mathrm{Ei}\left(-\frac{B}{t-t_0}\right) + 2AQ(t)s \quad \text{.....(6)}$$

where

$$A = \frac{\mu}{4\pi kH} \quad \text{and} \quad B = \frac{\phi\mu c r_w^2}{4k} \quad \text{.....(7)}$$

Equation (6) assumes radial flow in an infinite reservoir. The wellbore pressure at the beginning of the observation time interval is denoted by $p_{0w}=p(t_0)$, ϕ and c are the formation porosity and bulk compressibility. The skin factor s is equal to $\ln(r_w/r_{wb})$, where r_{wb} is the actual wellbore radius[14]. Parameter Q_{-1} is the effective injection rate corresponding to the near-wellbore steady-state formation pressure distribution resulting from operations prior to $t=t_0$. The wellbore pressure at $t=t_0$, p_{0w}, is computed using the Theis solution[16] over a substantial time period, and assuming undisturbed reservoir pressure as the initial condition. Note that p_{0w}, is not equal to the reservoir pressure due to the injection conducted prior to $t=t_0$.

In the simulations, we have assumed the reservoir pressure p_e equal to 950 psi and the ambient background quasi-steady-state injection rate Q_{-1} equal to 150 bbl/day. We used A=1. psi-day/bbl, B=0.001 day. These values of parameters A and B do not describe any specific formation, but have realistic orders of magnitude.

If the rate changes in steps, Fig. 4, the respective injection pressure is not a piecewise constant function of time Fig. 5. Nevertheless, the Hall plot, Fig. 6, is almost piecewise linear. The reason is that the solution is based on the exponential integral,

$$-\mathrm{Ei}\left(-\frac{B}{t-t_0}\right) \quad \text{.....(8)}$$

whose cumulative integral is close to a linear function. The "linearity" of a function of one variable can be "measured" by the magnitude of its second derivative. If this derivative is close to zero, then the function is almost linear. For the exponential integral (8), one has

$$\frac{d^2}{dt^2}\int_{t_0}^{t} -\mathrm{Ei}\left(-\frac{B}{\tau-t_0}\right) d\tau = -\frac{d}{dt}\mathrm{Ei}\left(-\frac{B}{t-t_0}\right) = \frac{\exp\left(-\frac{B}{t-t_0}\right)}{t-t_0} \quad (9)$$

Multiplication of both sides of the last equation by B makes it dimensionless

$$B\frac{d^2}{dt^2}\int_{t_0}^{t} -\mathrm{Ei}\left(-\frac{B}{t-t_0}\right) dt = \exp\left(-\frac{B}{t-t_0}\right)\frac{B}{t-t_0} \quad \text{....(10)}$$

The right-hand side of Eq. (10) is sandwiched between zero and $B/(t-t_0)$. The latter expression decays as $t-t_0$ grows. The parameter B is usually small, and the closeness of the cumulative integral of the exponential integral (8) to a linear function reveals itself clearly.

Fig. 2 and Fig. 3 show example calculations illustrating the comments about the exponential integral. Although the exponential integral (8) is not a constant function, Fig. 2, the plot of its cumulative integral versus time is almost a linear due to the decay of the second time derivative (10) with increasing t.

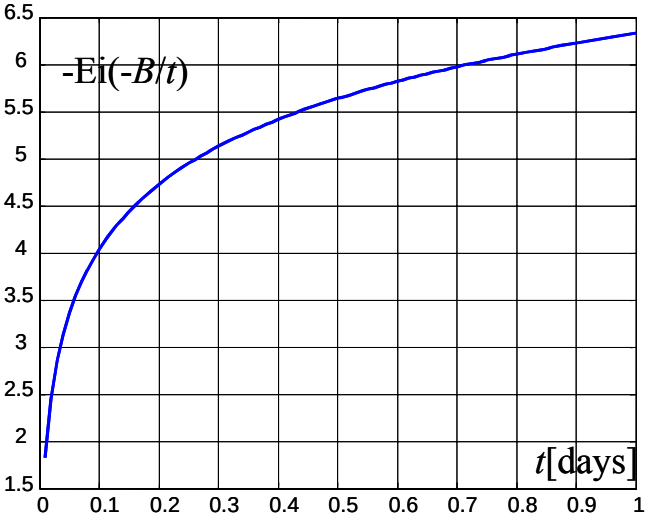

Fig. 2. Example: the plot of exponential integral (8) with B=0.001 [days]

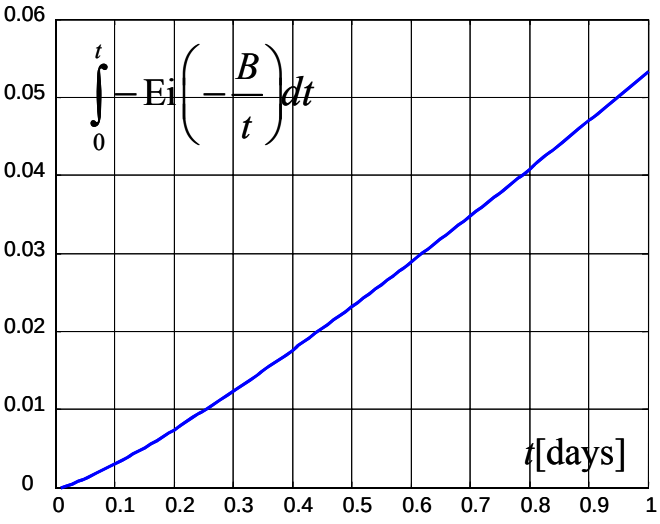

Fig. 3. Cumulative integral of the exponential integral (8). Although the function is not constant, Fig. 2, the cumulative integral is almost a linear function

Fig. 6 shows the Hall plot of the generated data. The plot is practically a straight line (red line) only if p_e in Eq. (4) is exactly equal to the value the reservoir pressure used in the simulations. If, instead of the exact value, an incorrect reservoir pressure is used in Eq. (4), the plot is a broken line (black and blue lines). The corners on the lines correspond to the moments when the injection rates are changed by a step increment. This picture is in full analogy with the illustration presented in Fig. 1,

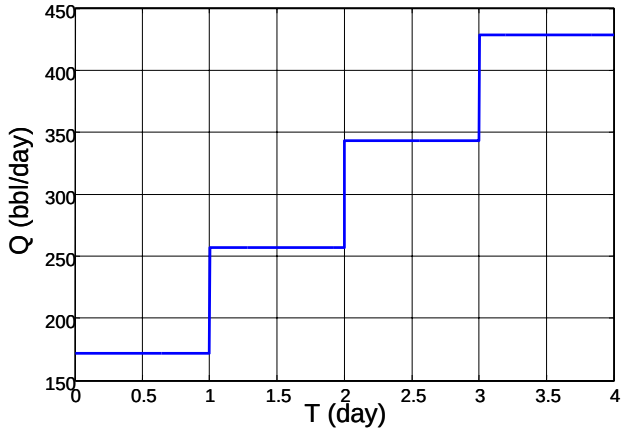

Fig. 4. Step increase of injection rate

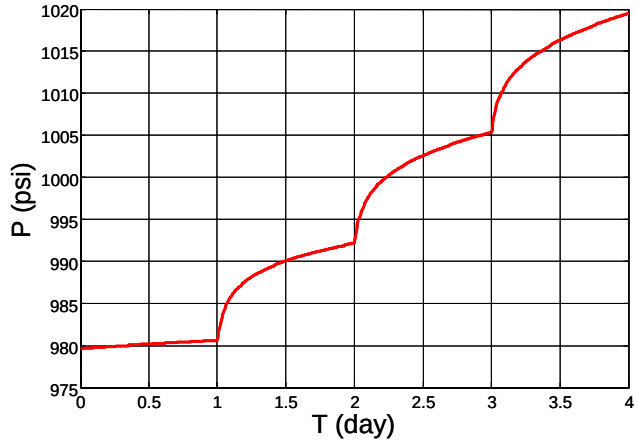

Fig. 5. Computed pressure buildup corresponding to the rates in Fig. 4.

Slope Plot: A New Well Diagnostic Tool

Visual inspection of Hall's plot can be deceiving. The integration filters out pressure and rate fluctuations, which are normally not too large in comparison with the respective mean values. In this section, we demonstrate that these visually almost imperceptible Hall plot slope variations can be analyzed to extract very important information about the effective reservoir pressure and well injectivity.

As we have demonstrated, the correct Hall plot requires knowledge of the mean ambient reservoir pressure p_e. This pressure cannot be measured, so we use in our analysis an "incorrect" Hall plot, with p_e set zero. To calculate the slope of this plot, one needs to evaluate the derivative

$$S = \frac{d\Pi}{dV} \quad \text{.....(11)}$$

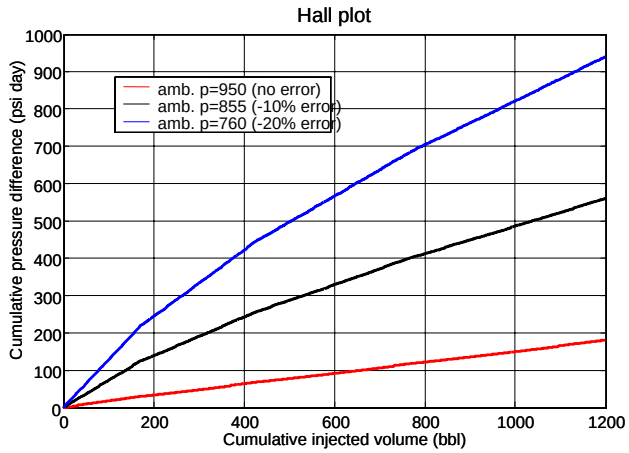

Fig. 6. Three versions of the Hall plot analysis of the data presented in Fig. 4 and Fig. 5. Only the exact reservoir pressure of 950 psi yields a straight line. Inaccurate information about the reservoir pressure results in slope breaks.

From Eq. (5),

$$S = \frac{p_w}{Q} \quad \text{.....(12)}$$

From Eqs. (1) and (3), at quasi steady-sate conditions,

$$S = \frac{p_e}{Q} + b \quad \text{.....(13)}$$

The latter equation implies that the plot of S versus $1/Q$ is a linear function. Injection rate Q and, by virtue of Eq. (12), the slope S are parameters available from measurement. Therefore, both the ambient reservoir pressure p_e and the well injectivity parameter b are obtained from Eq. (13) by linear fit of S versus $1/Q$. This procedure is abbreviated as the "slope plot analysis." Once p_e is estimated from the slope of the slope plot, it can be used to create the Hall plot according to Eq. (4).

Fig. 7 presents the slope plot analysis of the simulated data displayed in Fig. 4-Fig. 6. The plot is almost a straight line broken by the vertical jumps where the injection rate has step changes. These parallel displacements express changes in the injectivity parameter b. Since the formation properties do not change during these simulations, the variations of b are entirely due to the expansions of the influence zone radius caused by the increasing injection rate and pressure. The slope estimate of 957 psi is less than 1% different from the exact ambient pressure of 950 psi used in these simulations.

Like Hall's plot, the lines in Fig. 7 cannot be exactly straight because of the character of pressure variations in Fig. 5. However, these variations are not large in comparison with average injection pressure over the entire time interval. Therefore, visually, the lines are almost straight due to near-

linearity of the integral of the exponential integral function, as demonstrated by Eqs. (9)-(10).

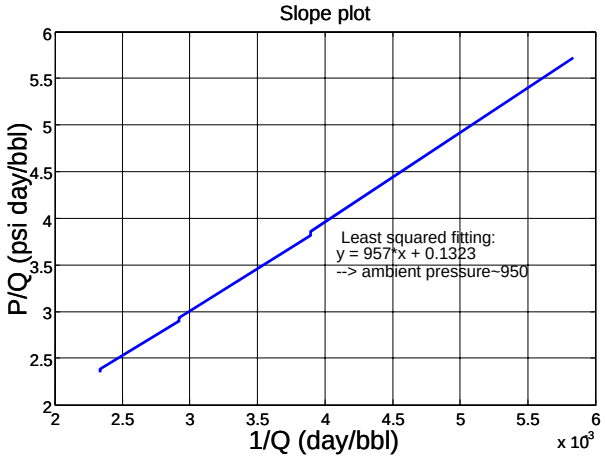

Fig. 7. Slope plot analysis of the forward simulations presented in Fig. 4--Fig. 6.

Seemingly, Eq. (1) can be used directly for linear fitting by substitution of the measured injection rates and pressures. However, practically, is more suitable for such analysis by the following reason. On the right-hand side of Eq. (1), the first term, the reservoir pressure, is usually larger than the second term, the additional pressure buildup due to fluid injection. This is why a linear fit of Eq. (13) in variables S and $1/Q$ is more stable than that of Eq. (1) in the original variables p_e and Q.

There is an important difference between how the Hall plot and the slope plot display the data. In a Hall plot, regardless of whether the correct reservoir pressure is used in Eq. (4) or not, the horizontal axis (cumulative injection) is a measure of elapsed time on injection: points to the right always correspond to later times than those to the left. Only if the well is shut down and Q=0, the points on the x-axis collapse. In a slope plot, time is not involved at all. Therefore, injection pressure – injection rate data points separated by substantial time can occur next to each other in a slope plot. In contrast, consecutive measurements can be separated from each other if, for example, there are abrupt fluctuations in the data. In the Hall plot, time-averaging of the data smoothes the curves. In a slope plot, time-averaging may actually complicate analysis and compromise the conclusions by introducing artificial "mean" data points.

Wells with a flow geometry different from radial flow, *e.g.* fractured wells, can be analyzed in a similar manner by replacing the exponential integral by a different well function. In fact, since slope analysis is based on the quasi-steady-state equation (13), it can be applied to any flow geometry with an appropriate modification of interpretation of coefficients b.

The computational example above simulates an idealized situation of perfectly steady-state flow in a homogeneous formation. In reality, these assumptions can hold true only on average. In fact, neighbor wells may interfere, the flow can be non-radial, *etc*. Our experience with analyzing data from injection wells in Lost Hills (see next section) shows that in most cases slope analysis produces an amazingly good straight line. Few outliers may indicate transient flow. If a systematic deviation occurs, it can be a sign of a problem. The character of this deviation can be used to diagnose the problem.

Parameter b in Eq. (1) is a lumped combination of the transmissivity, $T=kh/\mu$, and the logarithm of ratio of the radii, $\ln(r_e/r_w)$. If b is measured in psi-day/bbl, that corresponds to pressures measured in psi and injection rates measured in bbl/day, then

$$\frac{kH}{\mu \ln \frac{r_e}{r_w}} \left[\frac{\text{Darcy- ft}}{\text{cp}} \right] \approx 0.14 \frac{1}{b} \quad \text{.....(14)}$$

Thus, if b~0.14 [psi-day/bbl], r_w~0.3 ft, r_e~121 ft, then T~6 [Darcy-ft/cp]. If the injected fluid is water, μ~1 cp, and the reservoir thickness is about 120 ft, then the effective permeability of the rock is k=50 mD. Assuming 30% porosity and 20×10^{-6} psi^{-1} compressibility, the pressure diffusion at the distance 121 ft is of the order of one hour. Thus, for sound analysis, the measurements have to be collected over a time interval much larger than 1 hour. Since the information about reservoir rock properties is subject to high uncertainty, longer time observation intervals are recommended for more robust conclusions.

Detailed interpretation of the obtained estimates can be facilitated if additional information is available. For example, the formation transmissivity estimated from transient analysis[11, 12] can help to sharpen estimates of the radius of well influence. An example of such a calculation is presented in the next section.

Examples

Jim, please look if you can elaborate here and here

This work is a part of the development of automatic waterflood surveillance and control methods and software, and the integration of these tools with the Supervisory Control and Data Acquisition (SCADA) system in Lost Hills. Each water injection string is equipped with a flow meter and pressure gauge. The downhole injection pressure is calculated by adding the hydrostatic pressure to the midpoint of perforations to the gauge readings. The viscous pressure drop in tubing flow is neglected because of the low flow rates. In fact, even if this pressure drop were of importance, being proportional to the flow rate, it would be automatically accounted for through a small adjustment to the skin factor, or the coefficient b in Eq. (2).

Data from several injection wells at Lost Hills oil field are used in this section to illustrate the slope method. The pressures and rates are measured and automatically collected every minute. This high temporal resolution provides an excellent opportunity for the subsequent data analysis.

Fig. 8 and Fig. 9 display injection rates and injection pressures collected from well A over 6 days of regular operations. Except a spike on the fourth day, there are no significant fluctuations in the flow regime.

First, the starting four days of data were selected for the Hall plot analysis. The time interval was reduced to better illustrate the appearance of kinks in the plot caused by the injection rate change on the second day, Fig. 8. On a longer time interval, these kinks become less noticeable because the

cumulative pressure integral grows quickly and even significant fluctuations become hidden.

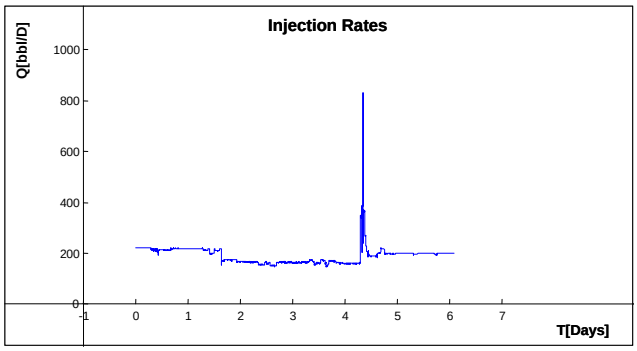

Fig. 8. Well A: Injection rate data collected over 6 days

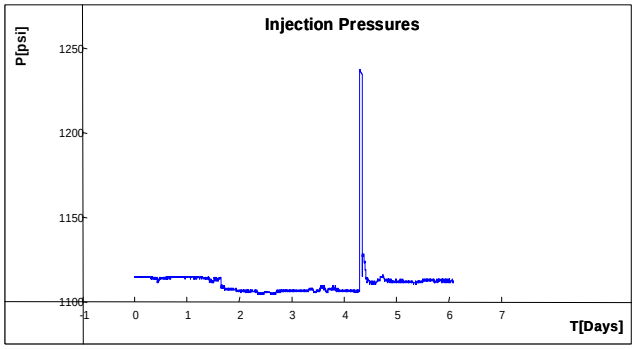

Fig. 9. Well A: Injection pressure over 6 days. The downhole pressure is calculated using the hydrostatic pressure increase.

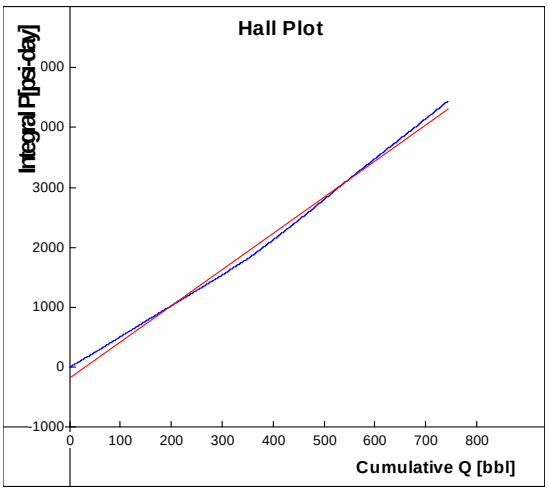

Fig. 10. Plot of the cumulative pressure versus cumulative injection volume neglecting the ambient reservoir pressure, i.e. p_e=0 in Eq. (4). The blue line is data and the red line is linear fit.

The plot in Fig. 10 (the blue line) consists of two straight segments and the change of the slope at the joint corresponds to approximately 400 barrels of cumulative injection. Comparison with Fig. 11 and, further, with Fig. 8 and Fig. 9 shows that this change of slope occurred when the flow rate dropped by approximately 50 bbl/day on the second day. It is tempting to conclude that the slope change in Fig. 10 is a sign that the near-wellbore formation may have sustained damage. However, we demonstrate below that it is not the case. The slope change in Fig. 10 is caused entirely by the incorrect application of Hall plot analysis resulting from the lack of information about the reservoir pressure, *cf.* examples in Fig. 1 and Fig. 6 above.

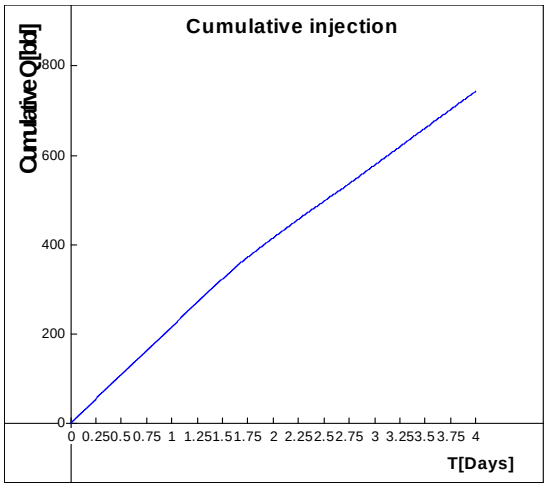

Fig. 11. Well A: The cumulative injection volume versus time.

Fig. 12 displays the result of slope analysis applied to the data shown in Fig. 8 and Fig. 9. With exception of very few outliers, the data points (blue circles) are closely aligned along the straight line 1075.56/Q+0.19 [psi-day/bbl] (the red line). Since the data in Fig. 12 do not involve time, neighbor points in the plot can be remote in time. To link the data to the time, Fig. 13 displays the plot of the inverse injection rate $1/Q$ versus t. The data points are grouped into four groups numbered by the roman numerals I, II, III, and IV. Groups I and IV, which are separated in time, merge into one group in Fig. 13. In contrast, Groups II and III are close in time but are separated in Fig. 13.

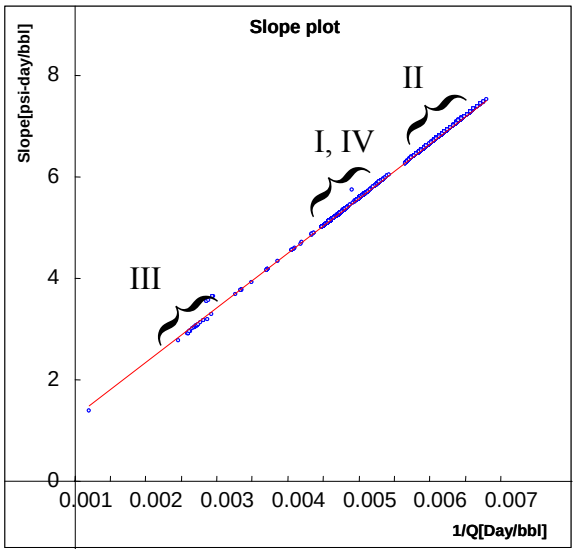

Fig. 12. Well A: The slope plot. The blue dots are data and the red line is linear fit. The ambient pressure estimate, i.e., the line slope is 1075.56 psi, and the intercept

b is 0.19 psi-day/bbl.

The reservoir pressure estimate of 1075.56 psi is an effective pressure that determines the reservoir "resistance" to the injection. This estimate characterizes the mean reservoir pressure along the boundary of the domain influenced by Well A. The presented analysis is insufficient to resolve the local pressure variations caused by reservoir heterogeneities. However, p_e, along with the coefficient b, carry important information about the pressure distribution in the reservoir. It can be used to monitor waterflood performance, assess possible reservoir compartmentalization, and determine well interactions with natural or induced fractures and faults. Analysis of the mean pressure maps in juxtaposition with the satellite subsidence images[3] can be used to set up sensible target rates for individual injectors[2]. Such an analysis will be discussed elsewhere.

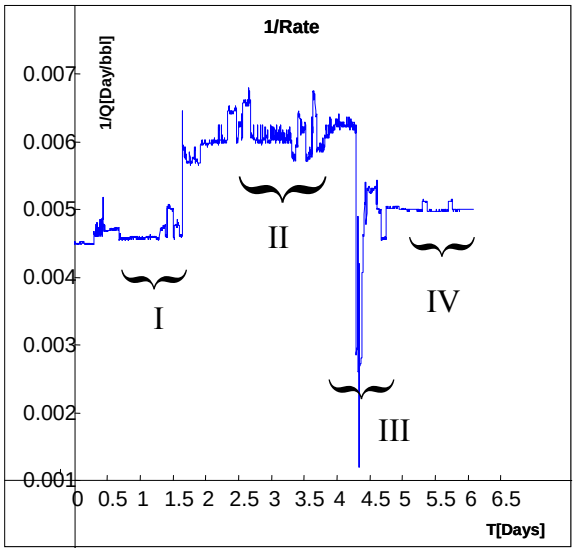

Fig. 13. Well A: The inverse injection rate, in day/bbl, versus time.

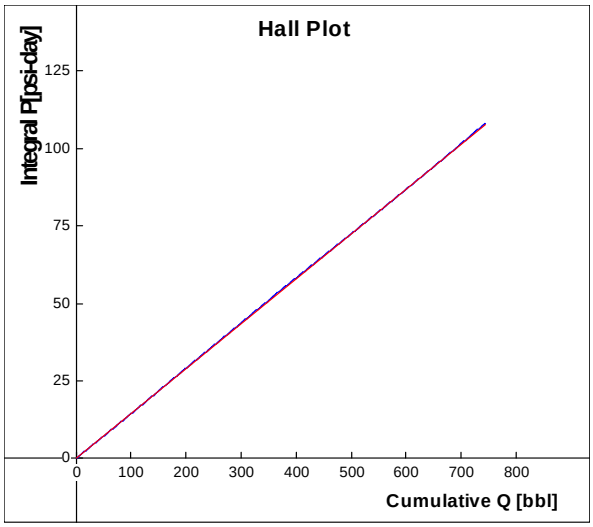

Fig. 14. Well A: The Hall plot after correction for the estimated ambient reservoir pressure. The blue line is based on the data and the red line is linear fit. The red and blue lines practically coincide.

Substitution of reservoir pressure estimates into the Hall plot using Eq. (4) makes it a practically straight line, see Fig. 14. Note that the range of values along the vertical axis in Fig. 14 is substantially smaller than that in Fig. 10. The reason is that pressure integration without deducting the reservoir pressure estimate results in operations with large numbers. Therefore, if the absolute value of the deviation between the straight red line and the plot in Fig. 10 were rescaled in terms of Fig. 14, this deviation would show up in a very explicit way. Thus, the absence of the slope change in Fig. 14 is due to the correct accounting for the ambient reservoir pressure in Eq. (4).

Application of the slope analysis to the data from well B, Fig. 15 and Fig. 16, provides an example of different kind. On the fourth day, after the missing data interval, injection rate had an abrupt fluctuation, after which, the rate continued to fluctuate near the same average value as during the first 3 days of injection. The pressures, however, slightly increased, starting from the 4th day. Visually, the plot of the pressure integral versus the cumulative injection is almost a straight line. The reason for this is that the fast growing pressure integral hides the fluctuations. After applying the slope analysis, effective reservoir pressure has been estimated at 1090 psi. This values has been substituted in Eq. (4), and the corrected Hall plot, Fig. 18 clearly shows an increase of the slope meaning a reduction of injectivity.

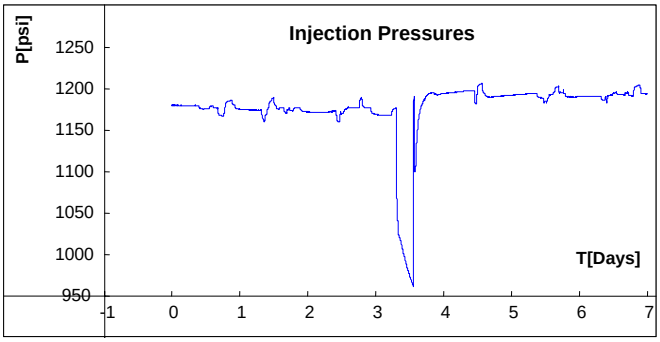

Fig. 15. Well B: The history of injection pressure. Note the pressure increment by the end of the 4th day of injection.

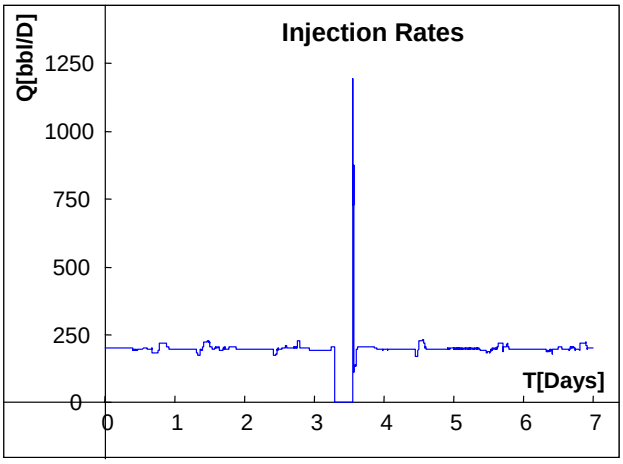

Fig. 16. Well B: The injection rate remains practically the same except lost data and a spike on the 4th day of

injection.

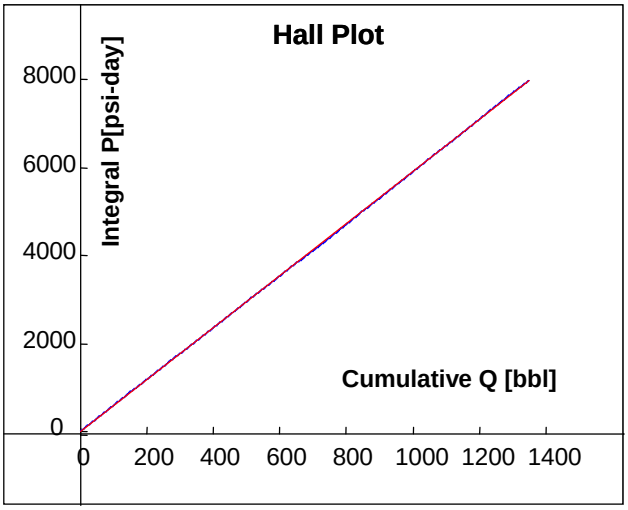

Fig. 17. Well B: The integrated pressure versus cumulative volume. The pressure increment after 4 days of injection is practically unnoticeable. The data (blue curve) and the fitting straight line (red) practically coincide.

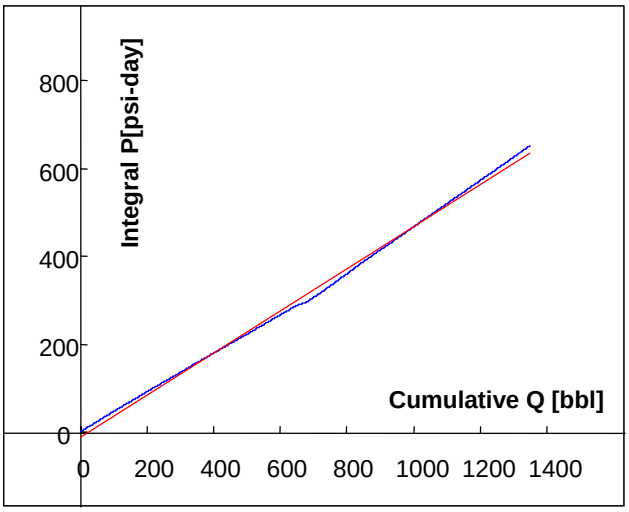

Fig. 18. Well B: The corrected Hall plot analysis: the injectivity reduction is clearly indicated by the increment of the slope.

The data from well C include a pressure fall-off curve due to the injection rate reduction from approximately 350 bbl/day to 200 bbl/day over the second and third days of injection, Fig. 19 and Fig. 20. The data presented in Fig. 19 and Fig. 20 can be analyzed using our transient analysis method[11,12]. This methods takes as input the injection rate and injection pressure data, and estimates the formation transmissivity, ambient reservoir pressure, and effective pre-test flow rate. The pre-test flow rate Q_{-1}, see Eq. (6), is a fitting parameter, but it can be used for an additional verification of the quality of fit.

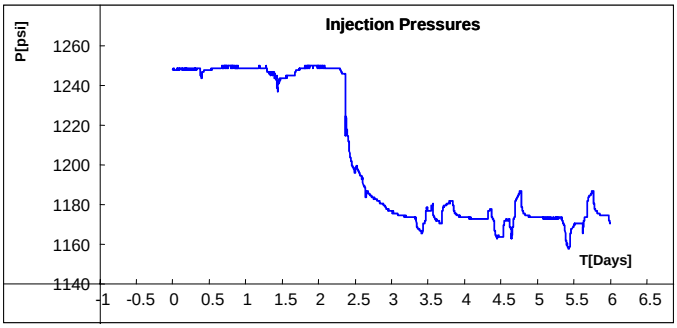

Fig. 19. Well C: A pressure fall-off curve amidst regular data.

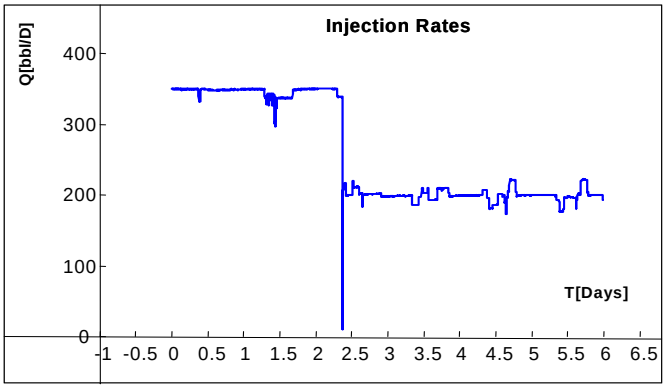

Fig. 20. Well C: An injection rate reduction.

The method[11,12] includes selection of the data interval to be analyzed, and a part of this interval where the pressure fitting will be performed. The data interval was selected between 25 and 125 hours of injection and its part starting at 45 hours was selected for the fitting. The red dotted curve in Fig. 21 is the result of fitting. The data are matched with high accuracy over a time period longer than 4 days. Additional confidence in the data fitting quality comes from the fact that the effective flow rate 25 hours before injection was estimated at 346 bbl/day, that is within 1% deviation from the actual mean injection rate over the first 25 hours of injection. In fact, multiple data analyses on different time intervals using ODA[17] produced consistent results. Over these multiple fitting runs, the mean estimate of transmissivity was about 1.46 Darcy-ft/cp and the ambient pressure was estimated at 1055 psi.

Fig. 22 shows the result of analysis of the same data from well C using the slope plot method. Although the data interval includes pressure transition, most of the data points (blue circles) are nicely aligned along a single straight matching line (red solid line). The group of outliers corresponds to the pressure fall-off, Fig. 19 and Fig. 21, where the flow is transient and, therefore, Eq. (1) is not satisfied exactly.

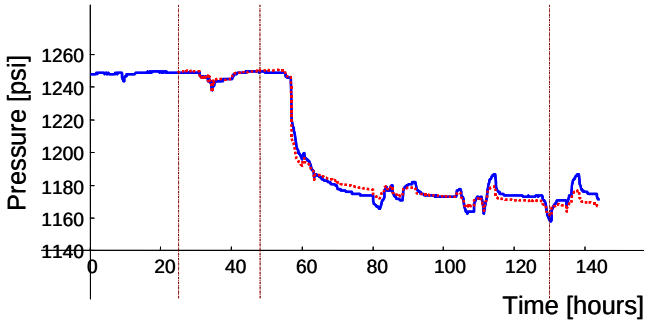

Fig. 21. Pressure curve fitting. The blue line are the data and the dotted red line is the fitting theoretical curve. The data between 25 and 125 hours of injection are used for analysis, the fitting is carried out on the time interval between 45 and 125 hours of injection. The fitting curve is extended to the right beyond 125 hours.

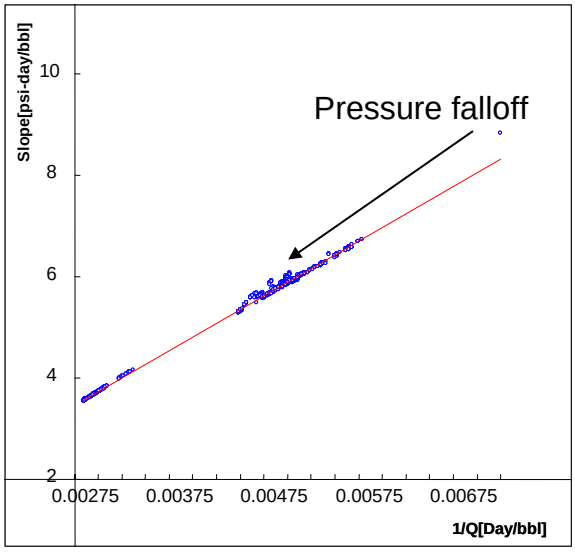

Fig. 22. The slope analysis yields the reservoir pressure estimate of 1078 psi and the intercept b=0.5 psi-day/bbl. The group of outlier data points corresponds to the pressure falloff, see Fig. 19 and Fig. 21.

Slope analysis yields an ambient pressure estimate of 1078 psi, that less than 3% different from the estimate of 1055 psi based on analysis of the falloff curve. Using Eq. (14) and the estimate of transmissivity obtained above, we infer that

$$\frac{r_e}{r_w} \approx 184 \quad \text{.....(15)}$$

If we assume the effective wellbore radius of 0.5 ft, then the influence radius is approximately equal to 92 ft. Note, that these estimates are average effective values and do not exclude significant local fluctuations of these parameters.

Conclusions

The Hall plot analysis of injection well performance requires knowledge of reservoir pressure at the outer boundary of the zone of influence of the well. Here the zone of influence of a well is defined as the region, where the reservoir pressure appreciably changes due to the injection. Neither the pressure at the boundary of the zone of influence nor the size of this zone is available from measurement. Therefore, the seeming simplicity of Hall's plot analysis is often deceiving. In particular, the change of slope of the Hall plot does not necessarily mean changing formation properties, but can be a consequence of the changing injection rate and pressure only.

A new method, called *slope analysis*, has been proposed. This method uses fluctuations of the slope of the plot of cumulative pressure versus cumulative injection volume to estimate the ambient reservoir pressure and injectivity. Therefore, the proposed analysis is based on data that are available from direct measurement and are routinely collected in waterflood operations. The obtained parameters are effective values representing average reservoir properties and do not exclude significant local deviations caused by the heterogeneity of the formation or well interference. The estimate of the reservoir pressure obtained using our slope plot can be used to correct the Hall plot.

The slope method has been tested and verified using simulated and field data. Using examples, we have shown that this analysis, based on the steady-state flow model, can be combined with transient analysis. The good agreement between the results obtained by both approaches brings confidence about the correctness of the results and the validity of the method in general. Joint inspection of the slope plot and transient analysis makes possible more accurate estimates, which cannot be obtained using each method separately.

The estimates of reservoir pressure obtained at each well can be mapped. Such a map in a project or at field scale provides valuable information about the reservoir conditions, including interactions between the wells and natural and induced faults, and reservoir compartmentalization. These pressure maps are discussed in detail elsewhere.

The results presented here are a part of the field-scale waterflood control in Lost Hills developed jointly by ChevronTexaco with participation of the University of California, Berkeley, and the Lawrence Berkeley National Laboratory. Incorporation of these results into injection control design will be discussed elsewhere.

Acknowledgments

The authors thank ChevronTexaco for the permission to publish this paper. The United States Department of Energy is acknowledged for partial support for this work provided under contract No. DE-ACO3-76FS00098 to the Lawrence Berkeley National Laboratory. First three authors appreciate partial support provided by ChevronTexaco, a member of the U.C. Oil® Consortium, University of California at Berkeley.

References

1.Talash, A.W., "An Overview of Waterflood Surveillance and Monitoring,". *Journal of Petroleum Technology*, 1988(December): p. 1539-1543.

2.Brink, J.L., T.W. Patzek, D.B. Silin, and E.J. Fielding. *Lost Hills Field Trial - Incorporating New Technology for Reservoir Management*. in *SPE Annual Technical Conference and Exhibition*. 2002. San Antonio, Texas: SPE.

3.Patzek, T.W., D.B. Silin, and E. Fielding. *Use of Satellite Radar Images in Surveillance and Control of Two Giant Oilfields in California. SPE71610*. in *2001 SPE Annual Technical Conference and Exhibition*. 2001. New Orlean, LA: SPE.

4.Earlougher, R.C., *Advances in Well Test Analysis*. Monograph Series. Vol. 5. 1977, New York: Society of Petroleum Engineers.
5.Patzek, T.W. and D.B. Silin. *Fluid Injection into a Low-Permeability Rock - 1. Hydrofrature Growth*. in *SPE/DOE Eleventh Symposium on Improved Oil Recovery*. 1998. Tulsa, Oklahoma: SPE, Inc.
6.Silin, D.B. and T.W. Patzek, "Water injection into a low-permeability rock - 2: Control model*,". Transport in Porous Media*, 2001. **43**(3): p. 557-580.
7.Silin, D.B. and T.W. Patzek, "Control model of water injection into a layered formation*,". SPE Journal*, 2001. **6**(3): p. 253-261.
8.Hall, H.N., "How to Analyze Waterflood Injection Well Performance*,". World Oil*, 1963(October): p. 128-130.
9.Buell, R.S., H. Kazemi, and F.H. Poettmann. *Analyzing Injectivity of Polymer Solutions With the Hall Plot SPE 16963*. in *SPE Annual Technical Conference and Exhibition*. 1987. Dallas, TX: SPE.
10.Honarpour, M.M. and L. Tomutsa. *Injection/Production Monitoring: An Effective, Method for Reservoir Characterization SPE20262*. in *SPE/DOE Seventh Symposium on Enhanced Oil Recovery*. 1990. Tulsa, OK: SPE.
11.Silin, D.B. and C.-F. Tsang, "A well-test analysis method accounting for pre-test operations*,". SPE Journal*, 2003(March): p. 22-31.
12.Silin, D.B. and C.-F. Tsang, "Estimation of Formation Hydraulic Properties Accounting for Pre-Test Injection or Production Operations*,". Journal of Hydrology*, 2002. **265**(1): p. 1-14.
13.Muskat, M., *The Flow of Homogeneous Fluids through Porous Media*. 1946, Ann Arbor, MI: J.W.Edwards, Inc.
14.Matthews, C.S. and D.G. Russell, *Pressure Buildup and Flow Tests in Wells*. 1967, New York, NY: SPE of AIME.
15.Silin, D.B., C.-F. Tsang, and H. Gerrish. *Replacing annual shut-in well tests by analysis of regular injection data: field-case feasibility study*. in *Underground Injection Science and Technology. Second International Symposium*. 2003. Berkeley, CA: LBNL.
16.Theis, C.V., "The Relationship Between the Lowering of the Piezometric Surface and the Rate and Duration of Discharge of a Well Using Ground-Water Storage*,". Transactions AGU*, 1935. **2**: p. 519-524.
17.Silin, D.B. and C.-F. Tsang, "ODA, Operations Data Analysis," . 2001, Lawrence Berkeley National Laboratory: Berkeley.

Nomenclature

A = fitting parameter, psi-day/bbl
B = fitting parameter, day
c = fluid/formation compressibility, psi^{-1}
H = reservoir thickness, ft
k = absolute rock permeability near the wellbore, Darcy
p_w = wellbore pressure, psi
p_e = average pressure in the formation, psi
p_{w0} = wellbore pressure at the beginning of data interval, psi
r_e = influence zone radius, ft
r_{wb} = wellbore radius, ft
r_w = effective wellbore radius, ft
Q = injection rate, bbl/day
Q_{-1} = pre-test injection/production rate, bbl/day
S = plot slope, psi
s = skin factor, dimensionless
ϕ = porosity, dimensionless
μ = fluid viscosity, cp

SI Metric Conversion Factors

acre	× 4.046 873	E+03 = m^2
Darcy	× 9.869	E-13 = m^2
bbl	× 1.589 873	E-01 = m^3
cp	× 1.0*	E-03 = Pa s
ft	× 3.048*	E-01 = m
ft^3	× 2.831 685	E-02 = m^3
in.	× 2.54*	E+00 = cm
md	× 9.869 233	E-04 = μm^2
psi	× 6.894 757	E+00 = kPa